Int. J. Heat Mass Transfer. Vol. 35, No. 6, pp. 1527–1532, 1992
Printed in Great Britain

0017–9310/92 $5.00+0.00

Buckling of a thermal plume

H. Q. YANG
CFD Research Corp., 3325-D Triana Blvd., Huntsville, AL 35805, U.S.A.

(*Received* 19 *February* 1991 *and in final form* 6 *May* 1991)

Abstract—The transition of a thermal plume from laminar to turbulent flow is characterized by a non-axisymmetric deformation. Past analyses are limited either to the planar plume or to the axisymmetric assumption, and subsequently are not capable of predicting the real phenomenon. The present study develops a new dispersion equation which accounts for the instability of all transverse modes on the plume. The dispersion equation shows that the dynamic interaction of the ambient air is responsible for the growth of any disturbance on the plume surface, and the sinuous mode has the highest growth rate at all wavenumbers when the density difference between the plume and the surrounding air is small. The present theory proves the snake form of onset instability of a plume.

INTRODUCTION

THE TRANSITION of a laminar flow to turbulent flow usually follows the initial instability of the laminar flow to the naturally occurring disturbances. Depending on the flow condition and geometries, the transition process may take different forms. As for a free plume, the instability character is usually very different from that of the plume which is adjacent to a surface. It is well known that free body flows are much less stable than those adjacent to the surface, since the surface damps disturbance. The disturbance mechanisms that are asymmetric across the midplane are usually less stable than those that are symmetric. Indeed, the commonly-observed 'meandering' deformation of cigarette smoke or thermal plume from a point heat source due to buoyancy (as shown in Fig. 1) illustrates one of the many transition roads. A previous analysis of plume instability was attempted by Pera and Gebhart [1], for the planar plume. They used the Tollmien–Schlichting theory of small disturbance and showed that the assumed 2-D planar base plume flow was less stable for a symmetric mode than for an asymmetric one. The analysis was repeated by Haaland and Sparrow [2], retaining two of the several terms excluded in the conventional approximation. Kimura and Bejan [3] have carried out a series of experiments on cigarette smoke and demonstrate that at the transition of a laminar buoyant plume to the turbulent flow the plume assumes a sinusoidal (meandering) shape with a characteristic wavelength scaling with the local plume diameter. Theoretically, they argue that the transition occurs when the time of viscous penetration normal to the plume becomes comparable with the minimum time period with which the plume can fluctuate as an unstable inviscid stream. Indeed, the striking similarity of the above deformation of a straight flow stream into a sinusoidal shape with the classical buckling of a solid elastic column (Euler buckling) has opened a new subfield in the frontiers of fluid mechanics research—'buckling flows' [4]. An excellent review and pictorial collection of the buckling flows are provided by Bejan [4, 5]. As a science by itself, the buckling flow has been recognized as an entirely different formulation of the onset instability in plume flow [6]. The purpose of this paper is to analyze the buckling of an axisymmetric plume from the point of transverse instability. The plume is modeled as a stream with uniform velocity, and the subsequent instability of the cylindrical vortex sheet is studied.

FORMULATION AND SOLUTION

Here we study the instability of an infinitesimal amplitude wave on an initially axisymmetric plume surface of infinite length. The plume is modeled as a free straight stream with a constant radius a, velocity U_1, and density ρ_1. The surrounding air is modeled with density ρ_2 and velocity U_2. The fluids are assumed to be incompressible and inviscid. If the system is subjected to a disturbance the instantaneous velocity ($\boldsymbol{u}_i$) and pressure (p_i) can be decomposed into two components, the mean ($\mathbf{U}_i$ and P_i) and disturbance ($\mathbf{u}_i$ and p_i) quantities

$$\boldsymbol{u}_i = \mathbf{U}_i + \mathbf{u}_i \quad i = 1, 2 \tag{1}$$

$$p_i = P_i + \mathrm{p}_i \quad i = 1, 2 \tag{2}$$

where subscripts 1 and 2 represent the quantities in the plume and the air, respectively. The flow motion is governed by the conservation of mass and momentum. By substituting the above quantities into the governing equations in the cylindrical coordinates r, θ and z, and neglecting the second-order non-linear terms, we obtain linearized disturbance equations of the form:

$$\nabla \mathbf{u}_i = 0 \tag{3}$$

$$\partial \mathbf{u}_i/\partial t + U_i\, \partial \mathbf{u}_i/\partial z = -1/\rho_i \nabla p_i. \tag{4}$$

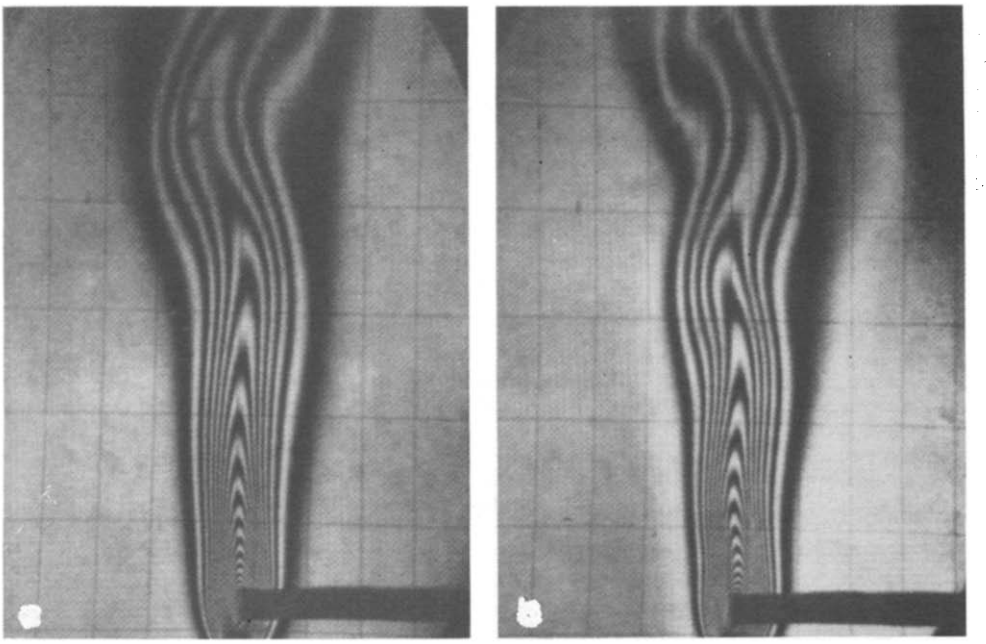

(a)

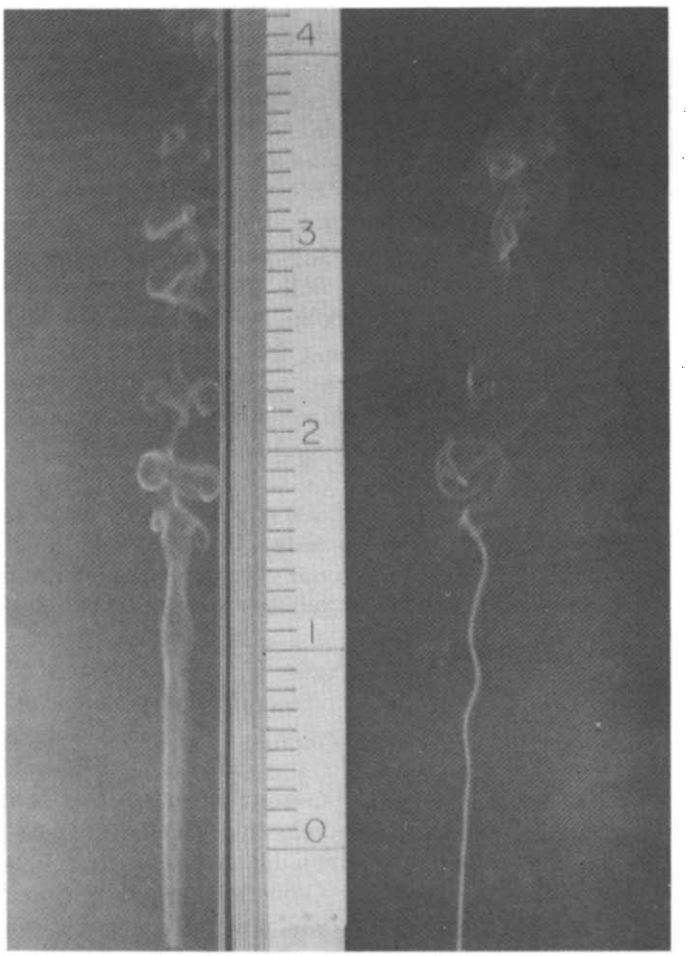

(b)

FIG. 1. Non-axisymmetric transition of thermal plumes. (a) Planar heat source. (b) Cigarette smoke.

By taking the divergence of equation (4) and making use of equation (3), we can eliminate the velocity vector, $\mathbf{u}_i$, and obtain a single equation for the perturbed pressure

$$\nabla^2 p_i = 0 \tag{5}$$

where

$$\nabla^2 = 1/r\,\partial/\partial r\,(r\partial/\partial r) + 1/r^2\,\partial^2/\partial\theta^2 + \partial^2/\partial^2 z. \tag{6}$$

Let the disturbance be three-dimensional with wavenumbers ka and m in the streamwise and azimuthal directions. The expressions for the perturbed quantities are

$$p_i = p_i(r)\,e^{i(kz+m\theta)+\alpha t} \tag{7}$$

$$\mathbf{u}_i = \mathbf{u}_i(r)\,e^{i(kz+m\theta)+\alpha t} \tag{8}$$

where α is the growth rate with respect to time. It is m in the above expressions that introduces the non-axisymmetric variation of the disturbance. Equation (5) now becomes

$$[1/r\,\partial/\partial r\,(r\,\partial/\partial r) - m^2/r^2 - k^2]p_i(r) = 0. \tag{9}$$

The solution to $p_i(r)$ is in terms of the mth order modified Bessel function of the first and second kinds

$$p_i(r) = C_{i1}I_m(kr) + C_{i2}K_m(kr). \tag{10}$$

Substituting equation (10) into equation (4), we can immediately find the velocity components

$$\mathbf{u}_i = -1/[\rho_i(\alpha+ikU_i)]\nabla[p_i(r)\,e^{i(kz+m\theta)+\alpha t}]. \tag{11}$$

There are four constants (C_{11}, C_{12}, C_{21} and C_{22}) that have to be determined from boundary conditions. For the plume ($i = 1$), the finite value of pressure at $r = 0$ requires

$$C_{12} = 0 \tag{12}$$

and similarly for the ambient air, the finite value of pressure at $r \to \infty$ requires

$$C_{21} = 0. \tag{13}$$

The other two constants are determined by the continuities of pressures and displacements on the interface

$$p_1 = p_2 \tag{14}$$

$$\eta_1 = \eta_2 \tag{15}$$

where η_1 and η_2 are the perturbed displacements of the interface of the two fluids, and they satisfy

$$v_i = \partial\eta_i/\partial t + U_i\,\partial\eta_i/\partial z \quad i = 1, 2. \tag{16}$$

v_i is the velocity component in the radial (r) direction. From equation (11) we have

$$v_1 = -C_{11}/[\rho_1(\alpha+ikU_1)]I'_m(kr) \tag{17}$$

$$v_2 = -C_{22}/[\rho_2(\alpha+ikU_2)]K'_m(kr). \tag{18}$$

Conditions (14) and (15) now become

$$C_{11}I_m(ka) - C_{22}K_m(ka) = 0 \tag{19}$$

$$C_{11}I'_m(ka)/[\rho_1(\alpha+ikU_1)^2] - C_{22}K'_m(ka)/[\rho_2(\alpha+ikU_2)^2] = 0. \tag{20}$$

The non-trivial solutions of the above equations exist if the determinant of the coefficient matrix vanishes. This condition leads to the following characteristic equation:

$$(\rho_{1m}+\rho_{2m})\alpha^2 + 2ik\alpha(\rho_{2m}U_2 + \rho_{1m}U_1) - k^2(\rho_{2m}U_2^2 + \rho_{1m}U_1^2) = 0 \tag{21}$$

where

$$\rho_{1m} = \gamma_m\rho_1, \quad \rho_{2m} = \beta_m\rho_2, \quad \gamma_m = kI_m(ka)/I'_m(ka),$$

$$\beta_m = -kK_m(ka)/K'_m(ka) \tag{22}$$

$$I'_m(ka) = dI_m(kr)/dr|_{r=a},$$

$$K'_m(ka) = dK_m(kr)/dr|_{r=a}. \tag{23}$$

RESULTS AND DISCUSSION

The solution of the quadratic equation (21) gives two roots

$$\alpha = ik(\rho_{1m}U_1 + \rho_{2m}U_2)/(\rho_{1m}+\rho_{2m}) \pm [k\rho_{1m}\rho_{2m}(U_1-U_2)^2]^{1/2}/(\rho_{1m}+\rho_{2m}). \tag{24}$$

It is clear that when the plume has the same velocity as the ambient, i.e. $U_1 - U_2 = 0$, it is neutrally stable. We further write equation (24) in a dimensionless form

$$\alpha^* = \pm(\alpha_r^*)_m + i(\alpha_i^*)_m \tag{25}$$

with

$$\alpha^* = \alpha a/|U_1 - U_2| \tag{26}$$

$$(\alpha_r^*)_m = ka(\gamma_m\beta_m Q)^{1/2}/(\gamma_m + \beta_m Q) \tag{27}$$

$$(\alpha_i^*)_m = \frac{-ka(\rho_{1m}U_1 + \rho_{2m}U_2)}{(\rho_{1m}+\rho_{2m})|U_1 - U_2|} \tag{28}$$

and Q as the density ratio

$$Q = \rho_2/\rho_1. \tag{29}$$

The axisymmetric mode is realized when $m = 0$. For any integer, $m > 0$, $(\alpha_r^*)_m$ represents the growth rate of a non-axisymmetric disturbance. Figure 2 shows the geometric representation of the transverse modes. For example, when $m = 0$ (Fig. 2(a)), the cross-section of the plume is circular and its radius varies only

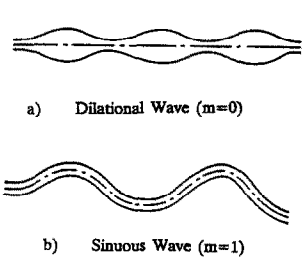

FIG. 2. Dilational wave and sinuous wave.

along the axial direction (z). The deformation of the plume is dilational and is sometimes called the varicose mode. This mode has been analyzed extensively by the existing mathematical theory on plume instability. For the mode with $m = 1$ (Fig. 2(b)), the cross-section of the plume is still nearly circular with constant size in the axial direction. The axis of the plume, however, is sinuous. This mode is commonly referred to as the sinuous mode or 'snake' mode. As for $m = 2$, the cross-section of the plume is elliptic [7]. When m becomes large, the development of the mth transverse mode leads to m peaks in the circumferential direction. To analyze the growth of the possible asymmetric modes, we will discuss several limiting as well as general cases.

Long wavelength limit

At the long wavelength limit

$$ka = 2\pi a/\lambda \to 0. \tag{30}$$

Since

$$\gamma_m = ka/[kaI_{m+1}(ka)/I_m(ka) + m],$$
$$\beta_m = ka/[kaK_{m+1}(ka)/K_m(ka) - m] \tag{31}$$

the limiting form of Bessel functions for I_m and K_m at $ka \to 0$ gives

$$\gamma_0 = 2/(ka), \quad \beta_0 = -ka \ln(ka) \quad \text{for} \quad m = 0 \tag{32}$$

$$\gamma_m = ka/m, \quad \beta_m = ka/m \quad \text{for} \quad m \neq 0. \tag{33}$$

Now, equation (27) is simplified to

$$(\alpha_r^*)_0 = ka[-2(ka)\ln(ka)Q]^{1/2}[2-(ka)^2\ln(ka)Q] \qquad m = 0 \tag{34}$$

$$(\alpha_r^*)_m = kaQ^{1/2}(1+Q) \qquad m \neq 0. \tag{35}$$

It is interesting to notice that the growth rate of an asymmetric mode is independent of m.

Short wavelength limit

When the wavelength of a disturbance is very short, or when $ka \to \infty$, the following two cases are discussed: (a) $m \ll ka$ and (b) $m \gg ka$.

(a) $m \ll ka$. For the transverse modes of $m \ll$ wavenumber ka, the values of γ_m and β_m in equation (31) reduce to

$$\gamma_m = 1, \quad \beta_m = 1. \tag{36}$$

Equation (27) now becomes

$$(\alpha_r^*)_m = kaQ^{1/2}(1+Q). \tag{37}$$

(b) $m \gg ka$. When the order of the modified Bessel functions (or the transverse mode m) is very high, the asymptotic expansion of the functions leads to

$$\gamma_m = ka/[(ka)^2+m^2)]^{1/2}, \quad \beta_m = ka/[(ka)^2+m^2]^{1/2}. \tag{38}$$

The dispersion relation of equation (27) now becomes

$$(\alpha_r^*)_m = kaQ^{1/2}/(1+Q). \tag{39}$$

We see that under both conditions the growth rates are the same and are independent of m. This is understandable because when $ka \to \infty$, the original cylindrical vortex sheet becomes a planar sheet.

Intermediate wavelength

For wavelengths which are neither very short nor very long, we can use equation (27) directly to compute the growth rate of the mth mode. It is observed from Fig. 3, which displays the growth rate for various modes at $Q = 1.0$, that the system is unstable at all wavenumbers for all modes, and asymmetric modes ($m > 0$) are more unstable than the symmetric one ($m = 0$). It seems that all asymmetric modes have almost the same growth rate. Careful examination of the calculated data indicates that the sinuous mode has the highest growth rate in all the modes, and the following relation holds:

$$(\alpha_r^*)_1 > (\alpha_r^*)_2 > (\alpha_r^*)_3 \cdots > (\alpha_r^*)_m \cdots > (\alpha_r^*)_0. \tag{40}$$

At limits of $k \to 0$ and $k \to \infty$, the growth rates for all the modes approach the asymptotic values discussed above.

Effect of density ratio

For the buoyancy flow, the density ratio reflects the dimensionless temperature ratio

$$Q = \rho_2/\rho_1 = T_1/T_2. \tag{41}$$

The density ratio also relates to the Grashof number. Since $\rho_2 > \rho_1$, Q is always larger than or equal to unity. If $\rho_2 \gg \rho_1$, the sinuous mode ($m = 1$) may not

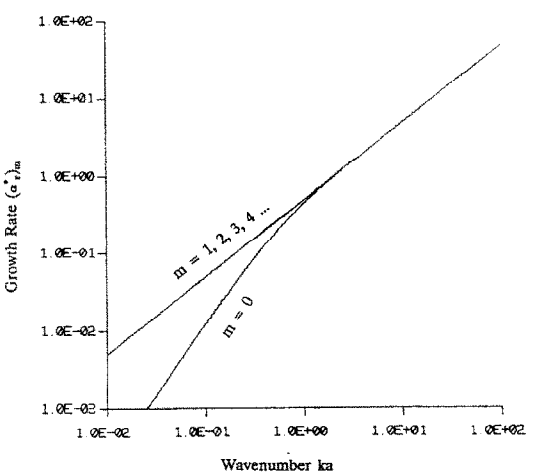

FIG. 3. Growth rate as a function of wavenumber at various transverse modes for $Q = 1.0$.

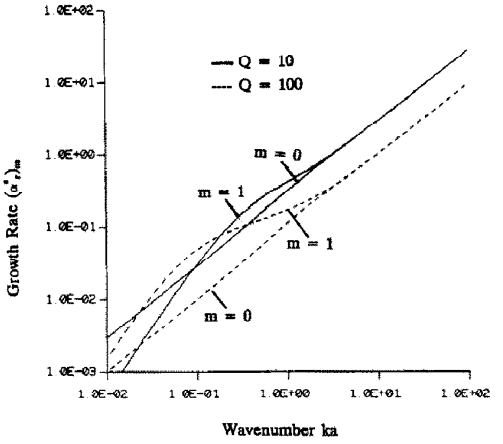

FIG. 4. Effect of density ratio for $m = 1$ and 0.

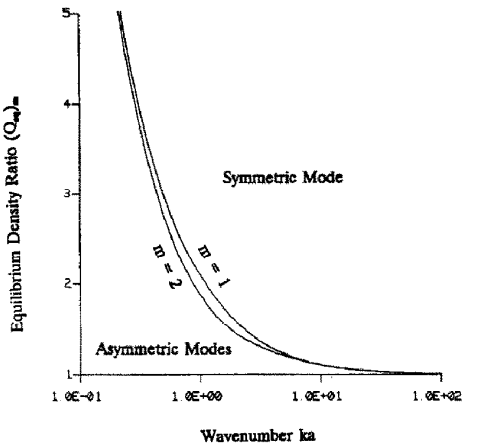

FIG. 6. Amplified view of Fig. 5 at $m = 1$ and 2.

be the preferred mode. This is proved by Fig. 4, which shows the growth rate of the dilational mode ($m = 0$) and the sinuous mode ($m = 1$) at the density ratios of $Q = 10$ and 100. Unlike the case of $Q = 1.0$, the symmetric mode dominates when the wavenumber is high. The wavenumber, above which $(\alpha_r^*)_0 > (\alpha_r^*)_1$, depends on density ratio. An equilibrium density ratio $(Q_{eq})_m$ is defined at which

$$(\alpha_r^*)_0 = (\alpha_r^*)_m. \tag{42}$$

From equation (27) we obtain

$$(Q_{eq})_m = [\gamma_0\gamma_m/(\beta_0\beta_m)]^{1/2}. \tag{43}$$

The calculations by the above relation show that for all m, $(Q_{eq})_m$ are almost the same and have the following relation:

$$(Q_{eq})_1 > (Q_{eq})_2 > \cdots > (Q_{eq})_m > \cdots. \tag{44}$$

The $(Q_{eq})_m$ are depicted in Fig. 5. An amplified view of Fig. 5 along with $(Q_{eq})_m$ is given in Fig. 6. As for cigarette smoke, in addition to a smaller radius of the plume, the density ratio is close to unity. Therefore, one expects sinuous instability. For the plume from a fire pool, both the radius of the plume and the density ratio are high (due to the high temperature of the flame). As a result, the dilational mode may be the least stable mode.

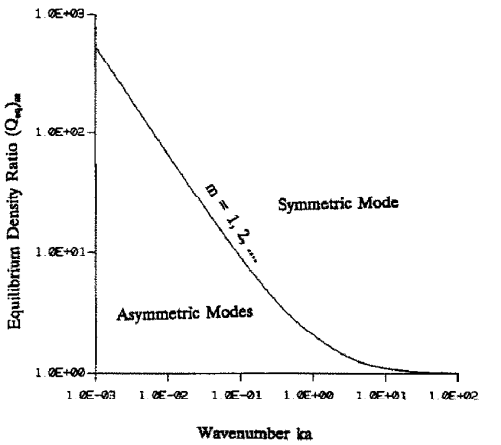

FIG. 5. Equilibrium density ratio as a function of wavenumber.

SUMMARY

The present paper derives a dispersion equation which accounts for the growth of all asymmetric modes in a plume. It is shown that when the density ratio between the plume and the surrounding air is small asymmetric modes have a higher growth rate than the symmetric one, and the sinuous mode is the most unstable mode. This proves theoretically the 'buckling' (or meandering) shape observed in the experiments.

REFERENCES

1. L. Pera and B. Gebhart, On the stability of laminar plumes; some numerical solutions and experiments, *Int. J. Heat Mass Transfer* **14**, 975–984 (1971).
2. S. E. Haaland and E. M. Sparrow, Stability of buoyant boundary layers and plumes, taking account of non-parallelism of the basic flows, *J. Heat Transfer* **95**, 295–301 (1973).
3. S. Kimura and A. Bejan, Mechanism of transition to turbulence in buoyancy plume flow, *Int. J. Heat Mass Transfer* **26**, 1515–1532 (1983).
4. A. Bejan, Buckling flows: a new frontier in fluid mechanics. In *Annual Review of Heat Transfer and Fluid Mechanics* (Edited by C. L. Tien), pp. 262–300 (1989).
5. A. Bejan, *Convection Heat Transfer*. Wiley, New York (1984).
6. B. Gebhart, Y. Jaluria, R. Mahajan and B. Sammakia, *Buoyancy-induced Flows and Transport*. Hemisphere, Washington, DC (1988).
7. H. Q. Yang, Non-axisymmetric breakup of a liquid jet during atomization, AIAA paper, AIAA-91-0693 (1991).

DEFORMATION D'UN PANACHE THERMIQUE

Résumé—La transition d'une panache thermique entre écoulements laminaire et turbulent est caractérisée par une déformation qui n'est pas axialement symétrique. Les analyses antérieures sont limitées soit au panache plan ou à l'hypothèse axisymétrique et par conséquent elles ne sont pas capables de prédire le phénomène réel. Cette étude développe une nouvelle équation de dispersion qui tient compte de l'instabilité de tous les modes transverses. L'équation de dispersion montre que l'interaction dynamique de l'air ambiant est responsable de la croissance d'une perturbation quelconque à la surface du panache et le mode sinueux a le taux de croissance le plus élevé à tous les nombres d'onde lorsque la différence de densité entre le panache et l'air environnant est faible. La théorie présentée prouve la forme sinueuse de l'apparition de l'instabilité d'un panache.

KRÜMMUNG EINER THERMISCHEN AUFTRIEBSFAHNE

Zusammenfassung—Der Übergang einer thermischen Auftriebsfahne von laminarer zu turbulenter Strömung ist durch eine nichtachsensymmetrische Deformation charakterisiert. Vorangegangene Analysen sind entweder auf ebene Auftriebsfahnen beschränkt oder auf die Annahme einer Achsensymmetrie. Daher sind diese Untersuchungen außerstande das tatsächliche Phänomen zu beschreiben. Hier wird nun eine neue Dispersionsgleichung entwickelt, die die Instabilität aller Übergangsarten der Auftriebsfahne berücksichtigt. Die Dispersionsgleichung zeigt, daß das dynamische Zusammenspiel mit der umgebenden Luft für das Wachstum jeglicher Störungen an der Oberfläche der Auftriebsfahne verantwortlich ist. Die Sinusform zeigt bei allen Wellenzahlen dann die größte Wachstumsrate, wenn der Dichteunterschied zwischen der Auftriebsfahne und der umgebenden Luft gering ist. Die vorgelegte Theorie bestätigt die Schlangenform für das Auftreten einer Instabilität der Auftriebsfahne.

ПРОДОЛЬНЫЙ ИЗГИБ ВОСХОДЯЩЕЙ СТРУИ

Аннотация—Переход восходящей струи от ламинарного режима к турбулентному характеризуется неосесимметричной деформацией. Предыдущие работы ограничивались либо плоскими, либо осесимметричными струями и не соответствовали реальной ситуации. В настоящем исследовании выведено новое уравнение дисперсии, учитывающее неустойчивость всех поперечных мод в струе. Уравнение показывает, что динамическое взаимодействие с окружающим воздухом обусловливает рост любых возмущений на поверхности струи и волнообразная мода обладает максимальной скоростью роста при любых волновых числах, если разность плотностей струи и окружающего воздуха незначительна. Согласно предложенной теории возникновение неустойчивозти струи характеризуется змеевидной формой.